[†]Present address: Whitehead Institute for Biomedical Research, 455 Main Street, Cambridge, MA, USA.
[‡]Present address: The University of Tokyo, Komaba Campus I, Build. 15, 3-8-1 Komaba, Meguro-ku, Tokyo 153-8902, Japan.
[§]Present address: Microbial Genetics Laboratory, Genetics Strains Research Center, National Institute of Genetics, 1111 Yata, Mishima, Shizuoka 411-8540, Japan.

THE ROYAL SOCIETY
PUBLISHING

Genetic defects in SAPK signalling, chromatin regulation, vesicle transport and CoA-related lipid metabolism are rescued by rapamycin in fission yeast

Kenichi Sajiki[1], Yuria Tahara[1], Alejandro Villar-Briones[1], Tomáš Pluskal[1,†], Takayuki Teruya[1], Ayaka Mori[1], Mitsuko Hatanaka[1], Masahiro Ebe[1], Takahiro Nakamura[1,‡], Keita Aoki[2,§], Yukinobu Nakaseko[2] and Mitsuhiro Yanagida[1]

[1]Okinawa Institute of Science and Technology Graduate University, 1919-1 Tancha, Onna-son, Okinawa 904-0495, Japan
[2]Graduate School of Biostudies, Kyoto University, Sakyo-ku, Kyoto 606-8501, Japan

KS, 0000-0001-7886-2979

Rapamycin inhibits TOR (target of rapamycin) kinase, and is being used clinically to treat various diseases ranging from cancers to fibrodysplasia ossificans progressiva. To understand rapamycin mechanisms of action more comprehensively, 1014 temperature-sensitive (ts) fission yeast (*Schizosaccharomyces pombe*) mutants were screened in order to isolate strains in which the ts phenotype was rescued by rapamycin. Rapamycin-rescued 45 strains, among which 12 genes responsible for temperature sensitivity were identified. These genes are involved in stress-activated protein kinase (SAPK) signalling, chromatin regulation, vesicle transport, and CoA- and mevalonate-related lipid metabolism. Subsequent metabolome analyses revealed that rapamycin upregulated stress-responsive metabolites, while it downregulated purine biosynthesis intermediates and nucleotide derivatives. Rapamycin alleviated abnormalities in cell growth and cell division caused by *sty1* mutants (Δ*sty1*) of SAPK. Notably, in Δ*sty1*, rapamycin reduced greater than 75% of overproduced metabolites (greater than 2× WT), like purine biosynthesis intermediates and nucleotide derivatives, to WT levels. This suggests that these compounds may be the points at which the SAPK/TOR balance regulates continuous cell proliferation. Rapamycin might be therapeutically useful for specific defects of these gene functions.

1. Introduction

Rapamycin is an antifungal metabolite discovered in the 1970s in *Streptomycin hygroscopicus*. It inhibits cell proliferation and antibody formation by T cells, which prompted its use as an immunosuppressive drug for organ transplantation (known by the generic name Sirolimus) [1]. Rapamycin forms a complex with peptidyl-prolyl-isomerase, FKBP12, to inhibit serine/threonine protein kinases designated TOR (target of rapamycin) [2–5]. TOR kinases comprise two distinct protein complexes inside cells that regulate cell proliferation [6]. Various studies have shown that many TOR pathway components are associated with cancer [7–10], and as a result, rapamycin has been used as an anti-tumour drug. Clinical trials have confirmed its effectiveness against mammary tumours, colon cancer, melanocarcinoma and ependymoblastoma [11]. In addition, rapamycin also extends the lifespans of yeast, fruit flies and mice [12–15], probably by reducing calorie consumption. Recently, rapamycin became the first drug in clinical trials for the treatment of fibrodysplasia ossificans progressiva, using patient-derived induced
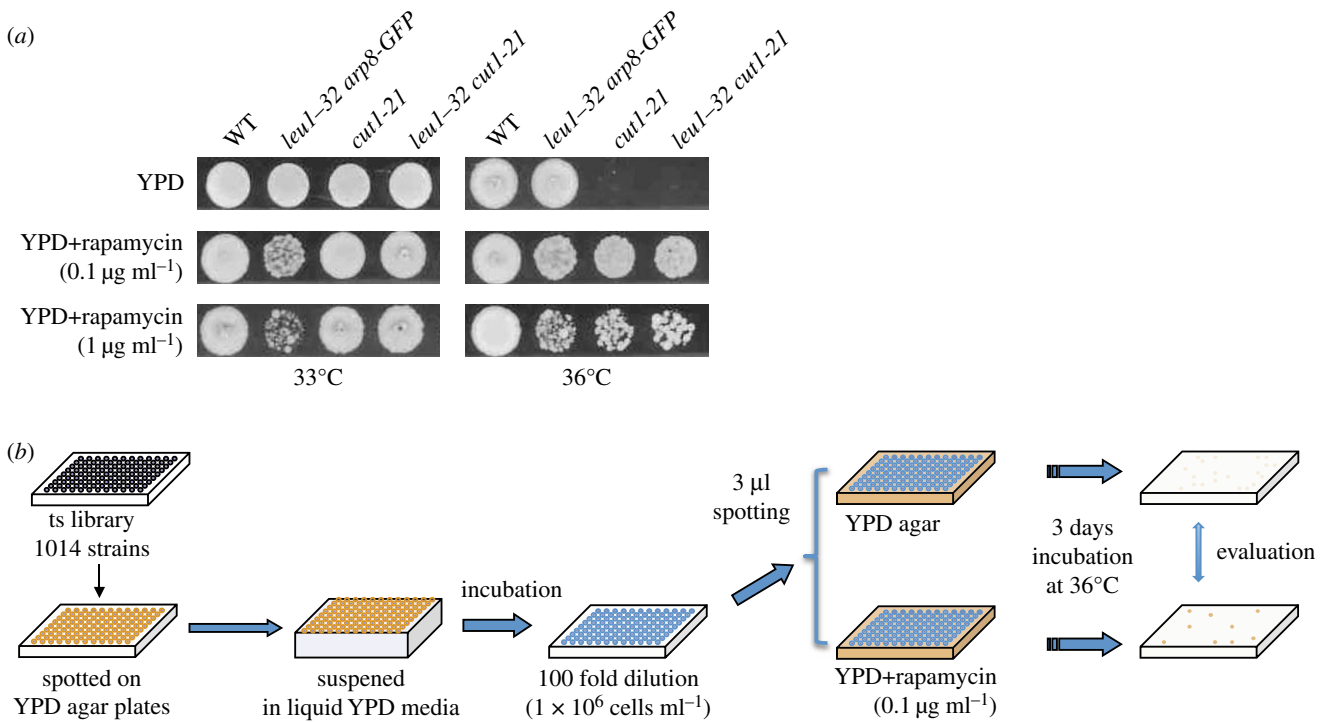
Figure 1. Screening of 1014 temperature-sensitive mutants yielded 45 strains in which the ts phenotype was rescued by rapamycin. (*a*) Spot tests of WT (h⁻ 972), parental strain (*leu1−32 arp8-GFP*), the previously reported *cut1-21* strain, on YPD plates with 0.1 μg ml⁻¹ rapamycin at 36°C clearly showed the rescue effect. (*b*) Schematized procedures of bulk screening using 96-well plates.

pluripotent stem cells [16]. Most recently, rapamycin has also proved effective in treating Pompe disease, which causes lysosomal glycogen accumulation in skeletal muscle and heart [17].

The fission yeast *Schizosaccharomyces pombe* has proved to be an excellent model for studying cellular functions of rapamycin and the TOR pathway, owing to the availability of genetic methods, comprehensive mutant libraries and high conservation of mammalian TOR pathway components [18]. In our previous report, we discovered that temperature sensitivity (ts) of *cut1*/separase and *cut2*/securin mutants was rescued by rapamycin, illuminating a new aspect of TOR signalling in cell growth and division [19]. This discovery suggested that there still exist undiscovered ts mutants that could offer a more comprehensive understanding of rapamycin. Accordingly, in the hope of discovering novel applications of this drug, we tested the capability of rapamycin to rescue mutants in our ts mutant library, which contains 1014 strains [20]. Mutants defective in 12 genes were found to be rescued by rapamycin. Among them, *sty1* mutants were further studied to show that rapamycin alleviated abnormal growth and division of these mutants. Also, we report a metabolome analysis to reveal the cellular impact of rapamycin. Metabolomic results strongly suggested that purine biosynthesis is implicated in the critical regulation targeted by rapamycin.

2. Results

### 2.1. Screening of the ts mutant library for rapamycin rescue

For library screening, a pilot spot test using a control strain (*cut1-21*) [19] showed that a rapamycin concentration of 0.1 μg ml⁻¹ was useful (figure 1*a*), because higher concentrations (e.g. greater than 1 μg ml⁻¹) inhibited growth of the parental strain of this library (*leu1-32 arp8-GFP*) at the restrictive temperature

(36°C). Therefore, using an automated robot system, screening was conducted by spotting 1014 ts mutants [20] onto YPD plates with or without 0.1 μg ml⁻¹ rapamycin (figure 1*b*). At 36°C, 62 strains showed better colony formation on YPD plates with rapamycin than without (electronic supplementary material, figure S1). These strains were further tested by serial dilution and manual spotting on plates to eliminate false positives (electronic supplementary material, figure S2). In 45 strains, it was confirmed that rapamycin rescued the ts phenotypes (figure 2*a*). Then, the mutated genes responsible for ts sensitivity were identified by suppression analysis and by either tetrad analysis or whole-genome sequencing (electronic supplementary material, table S1, Material and methods).

2.2. Rapamycin-rescued ts phenotypes of mutations in 12 genes

Among these 45 strains, 12 genes proved responsible for the ts phenotype (electronic supplementary material, table S1). They must be sole responsible genes for each strain, because plasmids containing WT genes for other background mutations could not rescue the ts phenotype. Based on reported functions, they belonged to four categories (figure 2*b*): stress-activated protein kinases (SAPK) (two genes), chromatin regulation (three genes), transport (four genes) and lipid metabolism (three genes).

The largest number of strains involved either of two SAPK mutants, *sty1* (MAPK; five strains) and *wis1* (MAPKK; five strains) (figure 2*a*). These genes are central to the stress-responsive signalling pathway, and Wis1 phosphorylates Sty1 [21,22]. Mutations in all *sty1* and *wis1* strains with amino acid substitutions were located in or near their protein kinase domains, and all with nonsense mutations (*sty1-791*, *wis1-887*, *sty1-989*) lacked the C-terminal half of the kinase domains (electronic supplementary material, table S1). Given their abundance, we examined these mutants further.
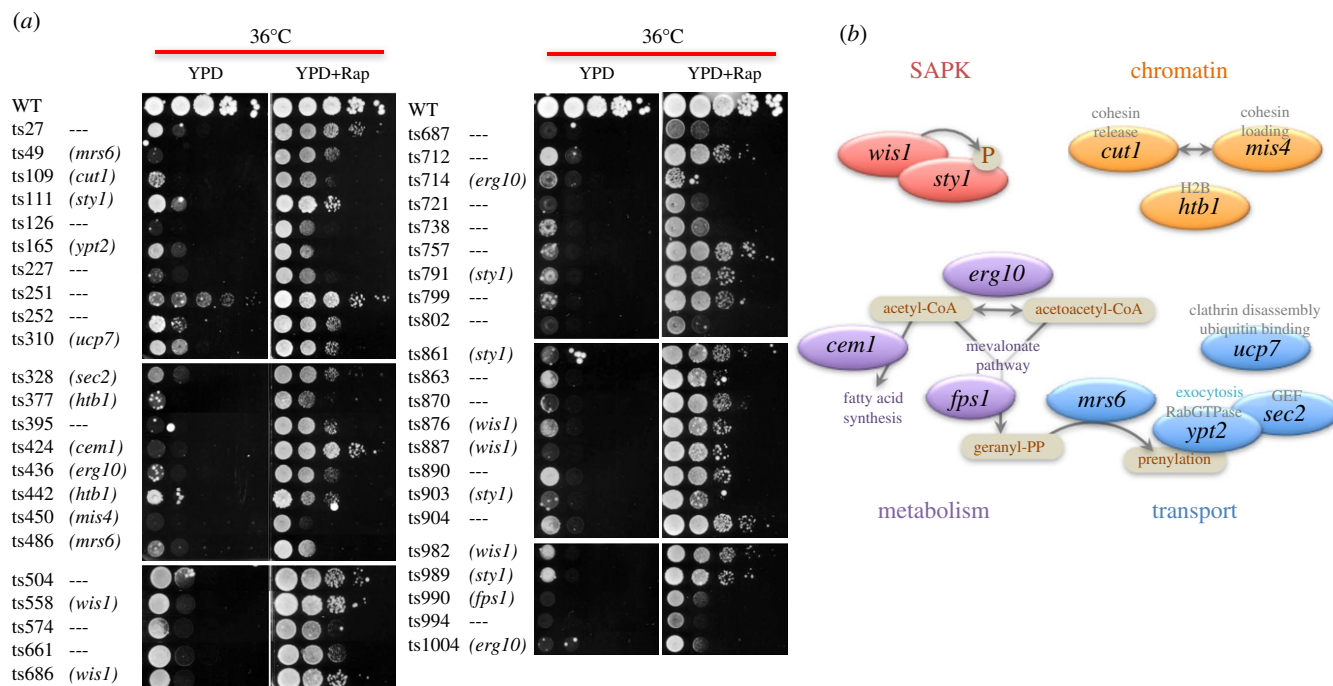
Figure 2. Twelve genes were responsible for the ts phenotypes of strains identified as responsive to rapamycin. (*a*) Spot tests of 45 strains on YPD or YPD + rapamycin (Rap) plates at 36°C. Names of responsible genes are in parentheses next to strain numbers. (*b*) The 12 responsible genes were classified into four groups, based on their reported cellular functions.

In the chromatin regulation gene group, one *cut1* mutant (*cut1-109*) was identified in addition to the previously reported *cut1-21* [19]. Cut1 cleaves Rad21, which is a subunit of cohesin complex. It should be noted that 18 other *cut1* mutants exist in this library, so further spot tests were performed for them. In fact, most of them revealed a more temperature-sensitive phenotype, which was also rescued by rapamycin (electronic supplementary material, figure S3A). Mutation sites were concentrated in Cut1's peptidase and central domains (electronic supplementary material, figure S3B). Other chromatin regulation genes included *mis4*, a cohesion loader for establishing sister chromatid cohesion [23,24], and *htb1*, a histone H2B (figure 2*c*). Four other *htb1* mutants have been identified in this library. Of those, two were mutated at the N-terminus: *htb1-377* (G30D) and *htb1-442* (E35 K) and showed the rescue phenotype, while *htb1-72* (G52D) and *htb1-223* (P102 L) did not [25]. The N-terminal end of H2B is phosphorylated under stressful conditions [26,27], suggesting the basis for this allelic difference.

In the vesicle transport gene group, one clathrin-binding gene (*ucp7*), one exocytic Rab-type GTPase gene (*ypt2*) and its GTP exchange factor (*sec2*), and one Rab geranylgeranyl transferase-related gene (*mrs6*) were identified (figure 2*b*).

In the metabolism gene group, there were three genes related to CoA metabolism and the mevalonate pathway: *erg10* (acetyl-CoA C-acetyltransferase), *cem1* (3-oxoacyl-[acyl-carrier-protein]-synthase condensing enzyme) and *fps1* (farnesyl diphosphate synthase) (figure 2*b*).

2.3. Rapamycin-induced cell division at 36°C, in contrast to SAPK mutations

All SAPK ts mutants showed identical phenotypes, and we also found a deletion strain of *sty1* (Δ*sty1*) that was similar. As with ts mutants, the Δ*sty1* strain showed reduced viability at 36°C, which was rescued by rapamycin (figure 3*d*). Therefore, Δ*sty1* was used to study functional

implications of SAPK and rapamycin, in order to eliminate potential dominant negative effects of ts mutants.

At the permissive temperature, 26°C, Δ*sty1* cells multiply slightly more slowly than WT, displaying longer cell lengths (figure 3*a,b,e*). At 26°C, addition of 200 nM rapamycin did not have a significant effect upon the rate of cell division, a negative result reported previously [28]. At 36°C, Δ*sty1* showed a ts phenotype with retarded mitotic increase, while WT cells divided much more rapidly (figure 3*a,b*). At this temperature, rapamycin rescued the ts phenotype of Δ*sty1*, accelerating cell division approximately 1.63-fold (figure 3*b*). Similar effects were also observed in the ts strain, *sty1-989* (electronic supplementary material, figure S4).

2.4. Rapamycin-rescued nuclear abnormality and viability loss of the SAPK mutant, Δ*sty1*, at 36°C, even under nitrogen deprivation

Cell morphology of Δ*sty1* was further examined at 36°C. Six hours after the temperature shift, cell size was abnormally elongated and septated cells were frequently observed (figure 3*e*). Also, nuclei appeared enlarged and deformed in Δ*sty1*. Such deformation was moderated by rapamycin. In fact, subsequent FACS analysis of Δ*sty1* showed that its 2C DNA peak expanded to the right at 36°C, but this expansion was alleviated when rapamycin was added (figure 3*f*). Thus, Sty1 and rapamycin may maintain proper nuclear and cell shapes at 36°C.

Previously, we reported that SAPK mutants showed abnormally expanded nuclei and severely decreased viability after nitrogen deprivation (−N) [29], so we tested whether rapamycin could also rescue this phenotype. After −N, WT cells undergo two divisions without cell growth, resulting in a roughly fourfold increase in cell number. G0 phase cells are small and round, and most have 1C DNA content (figure 3*g,i,j*). They complete G0 phase entry within 24 h after −N, and maintain high viability (figure 3*h*). However, Δ*sty1*
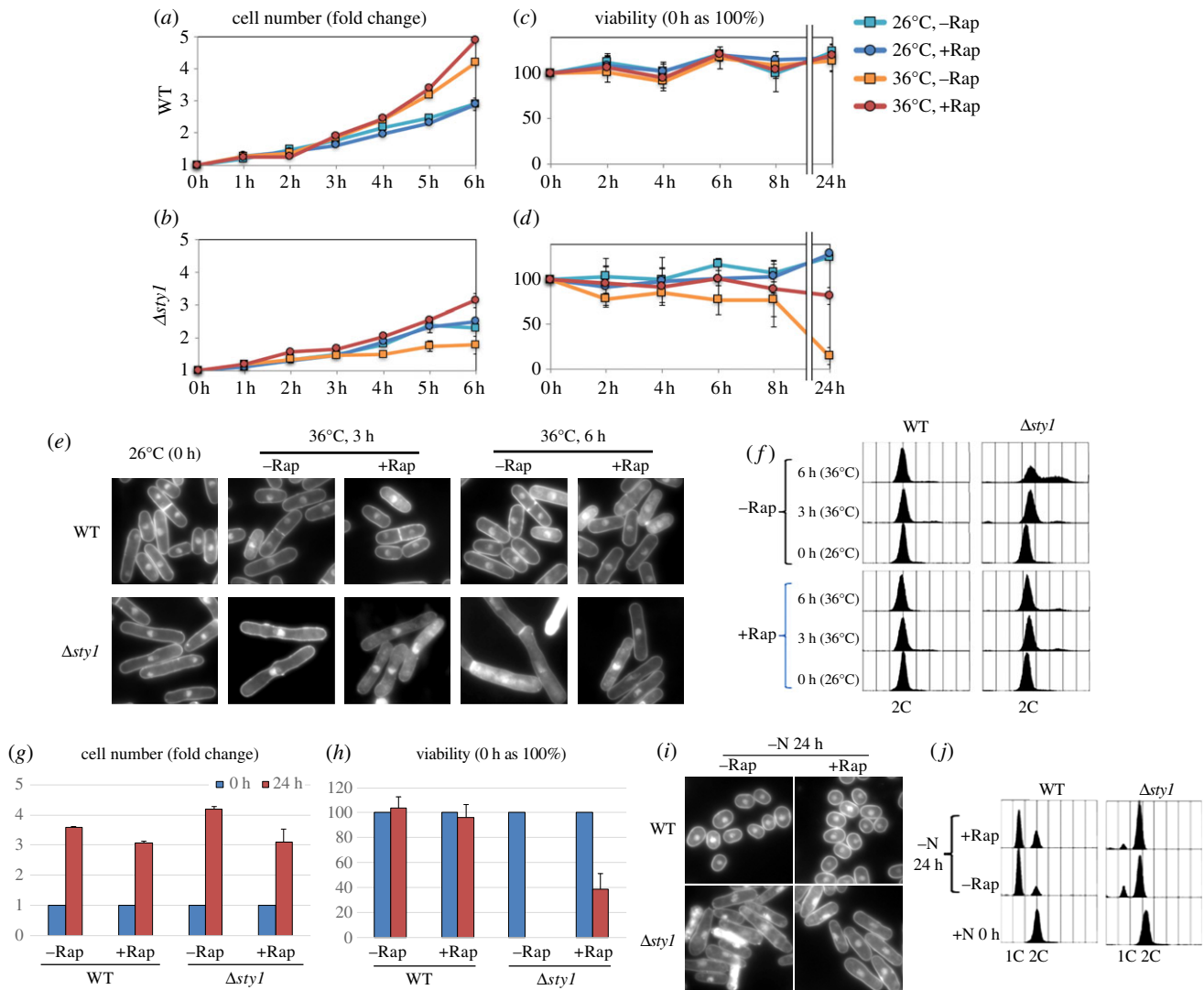
Figure 3. Rapamycin rescued abnormal cell division, growth and DNA content in $\Delta sty1$ mutants. ($a-d$) Cell number increment and viability of WT and $\Delta sty1$ in EMM2 liquid medium with or without 200 nM rapamycin at 26°C or 36°C were plotted in a time course. Error bars showed standard deviation. (e) DAPI images of WT and $\Delta sty1$ cells under the conditions indicated. (f) DNA content of WT and $\Delta sty1$ cells under the indicated conditions. (g,h) Cell number increment (g) and viability (h) of WT and $\Delta sty1$ before and 24 h after nitrogen deprivation ($-$N) in media with or without 200 nM rapamycin. Error bars showed standard deviation. (i) DAPI images of WT and $\Delta sty1$ cells at 24 h after $-$N in media with or without 200 nM rapamycin. (j) DNA content of WT and $\Delta sty1$ before and 24 h after $-$N in media with or without 200 nM rapamycin.

mutant cells could not stop cell growth or division after $-$N, increasing in number by about 4.3-fold. Cells were elongated with 2C DNA content (figure 3g,i,j). This demonstrates a clear failure of G0 phase entry, and cells lost all viability 24 h after $-$N (figure 3h), as with ts mutants reported previously [29]. When rapamycin was added to $\Delta sty1$, however, cell number increment after $-$N was suppressed to the WT level, and viability recovered by 39% (figure 3g,h). Interestingly, this rescue occurred without rescuing the elongated cell shape and 2C DNA content (figure 3i,j), implying cell morphology and viability are separately regulated under $-$N.

2.5. Rapamycin induces stress-responsive metabolites and basic amino acid derivatives at 36°C
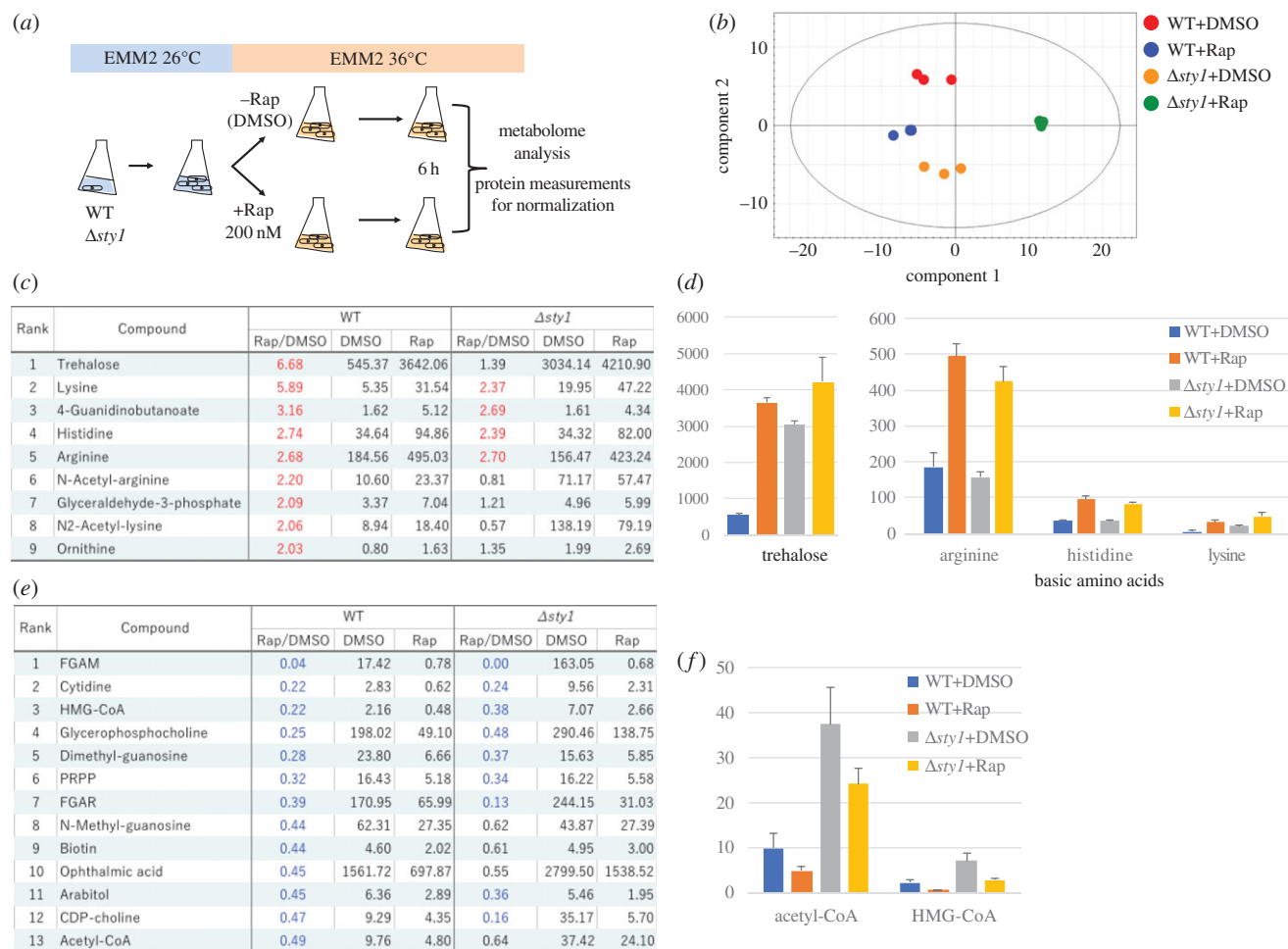
In order to examine effects on metabolism induced by rapamycin, we conducted quantitative metabolomic analysis of WT and $\Delta sty1$ cell cultures incubated for 6 h at 36°C with or without 200 nM rapamycin, the smallest concentration able to inhibit TOR signalling [28] (figure 4a). Since cell size varied among strains and conditions, data were normalized by protein concentration (electronic supplementary material, table S2).

The experiment was run in triplicate and reproducibility was confirmed using principal components analysis (figure 4b).

In WT, compared with DMSO (the solvent used for rapamycin, as a control), rapamycin increased nine metabolites greater than twofold (figure 4c). Those metabolites were trehalose, basic amino acids and their acetylated forms (arginine, histidine, lysine, N-acetyl-arginine, N-acetyl-lysine, 4-guanidinobutanoate, ornithine), and glyceraldehyde-3-phosphate. Trehalose, which showed the greatest increase, is well known as a stress-responsive metabolite [30]. Interestingly, it was also significantly induced in WT by rapamycin addition, but in $\Delta sty1$, the trehalose level was already high before rapamycin addition (figure 4d), implying that Sty1 might control stress response before adding rapamycin. WT and $\Delta sty1$ both increased basic amino acid titres after rapamycin addition (figure 4d).

2.6. Rapamycin reduces purine biosynthetic intermediates, nucleotide derivatives and CoA related metabolites at 36°C

In WT, rapamycin caused 13 metabolites to decrease to less than half (figure 4e). The majority of these were purine

(a)

(b)

(c)

Rank	Compound	WT			Δsty1		
		Rap/DMSO	DMSO	Rap	Rap/DMSO	DMSO	Rap
1	Trehalose	6.68	545.37	3642.06	1.39	3034.14	4210.90
2	Lysine	5.89	5.35	31.54	2.37	19.95	47.22
3	4-Guanidinobutanoate	3.16	1.62	5.12	2.69	1.61	4.34
4	Histidine	2.74	34.64	94.86	2.39	34.32	82.00
5	Arginine	2.68	184.56	495.03	2.70	156.47	423.24
6	N-Acetyl-arginine	2.20	10.60	23.37	0.81	71.17	57.47
7	Glyceraldehyde-3-phosphate	2.09	3.37	7.04	1.21	4.96	5.99
8	N2-Acetyl-lysine	2.06	8.94	18.40	0.57	138.19	79.19
9	Ornithine	2.03	0.80	1.63	1.35	1.99	2.69

(d)

(e)

Rank	Compound	WT			Δsty1		
		Rap/DMSO	DMSO	Rap	Rap/DMSO	DMSO	Rap
1	FGAM	0.04	17.42	0.78	0.00	163.05	0.68
2	Cytidine	0.22	2.83	0.62	0.24	9.56	2.31
3	HMG-CoA	0.22	2.16	0.48	0.38	7.07	2.66
4	Glycerophosphocholine	0.25	198.02	49.10	0.48	290.46	138.75
5	Dimethyl-guanosine	0.28	23.80	6.66	0.37	15.63	5.85
6	PRPP	0.32	16.43	5.18	0.34	16.22	5.58
7	FGAR	0.39	170.95	65.99	0.13	244.15	31.03
8	N-Methyl-guanosine	0.44	62.31	27.35	0.62	43.87	27.39
9	Biotin	0.44	4.60	2.02	0.61	4.95	3.00
10	Ophthalmic acid	0.45	1561.72	697.87	0.55	2799.50	1538.52
11	Arabitol	0.45	6.36	2.89	0.36	5.46	1.95
12	CDP-choline	0.47	9.29	4.35	0.16	35.17	5.70
13	Acetyl-CoA	0.49	9.76	4.80	0.64	37.42	24.10

(f)

Figure 4. Metabolome analysis revealed the cellular impact of rapamycin in WT and Δsty1. (a) Schematized procedures of metabolome analysis. (b) Principal components analysis (PCA) was conducted for the entire dataset of 98 metabolites (electronic supplementary material, table S2). A scatter plot of scores of the two principal components was shown. (c) List of metabolites that increased greater than twofold in a WT sample with rapamycin (Rap) compared with a control DMSO sample (DMSO). The DMSO and Rap columns show normalized peak areas and Rap/DMSO column shows the fold change. (d) Normalized mean peak areas with standard deviations of trehalose and basic amino acids in WT and Δsty1 with DMSO or Rap. (e) List of metabolites that decreased more than 50% in a WT sample with Rap compared with DMSO. (f) Normalized mean peak areas with standard deviations of acetyl-CoA and HMG-CoA in WT and Δsty1 with DMSO or Rap.

biosynthesis intermediates (FGAM, FGAR, PRPP) and nucleotide-related metabolites (cytidine, mimethyl-guanosine, N-methylguanosine, CDP-choline). They accounted for more than half of the decreased metabolites, implying that nucleotide metabolism is a major target of rapamycin.

Beside nucleotide derivatives, HMG-CoA and acetyl-CoA decreased by 78% and 51%, respectively (figure 4f). As mentioned above, another major group of mutants rescued by rapamycin is involved in CoA metabolism (figure 2b). Inhibition of the CoA pathway by rapamycin may be the basis for rescuing such mutants.

2.7. In the SAPK mutant, Δsty1, rapamycin abolished overproduction of purine biosynthesis intermediates and nucleotide derivatives

Metabolomic results indicated that many metabolites were overproduced in Δsty1 cells. In those cells, 37 metabolites were found at concentrations greater than twofold the level seen in WT cells (figure 5a, DMSO; electronic supplementary material, table S2). However, with rapamycin addition, most of these overproduced metabolites returned to WT levels, and only 11 remained greater than twofold (figure 5a, Rap; electronic supplementary material, table S2). Among those adjusted to WT level by rapamycin,

those that decreased more than 50% included biosynthesis intermediates (FGAM, SAICAR; figure 5c) and nucleotide derivatives (CDP, CDP-choline, CDP-ethanolamine, CTP, GDP, GDP-glucose, GTP, UTP; figure 5d). This implies that purine biosynthesis and nucleotide metabolism might be key regulatory targets of SAPK and rapamycin.

On the other hand, only three metabolites in Δsty1 decreased to less than 50% of the WT (figure 5b, DMSO; electronic supplementary material, table S2). Those were ergothioneine and methylated histidines, which could be related to stress response. When rapamycin was added, three more metabolites in Δsty1 decreased to less than 50% of the WT (figure 5b, Rap; electronic supplementary material, table S2). Again, two were purine biosynthesis intermediates (AICAR, FGAR), further suggesting that the purine pathway could be rapamycin's physiological target.

3. Discussion

In this study, we identified mutants in which the ts phenotype was rescued by rapamycin. Although roles of TOR have been reported in diverse cellular processes from protein synthesis to autophagy [6], the 12 genes identified here were rather narrowly focused.
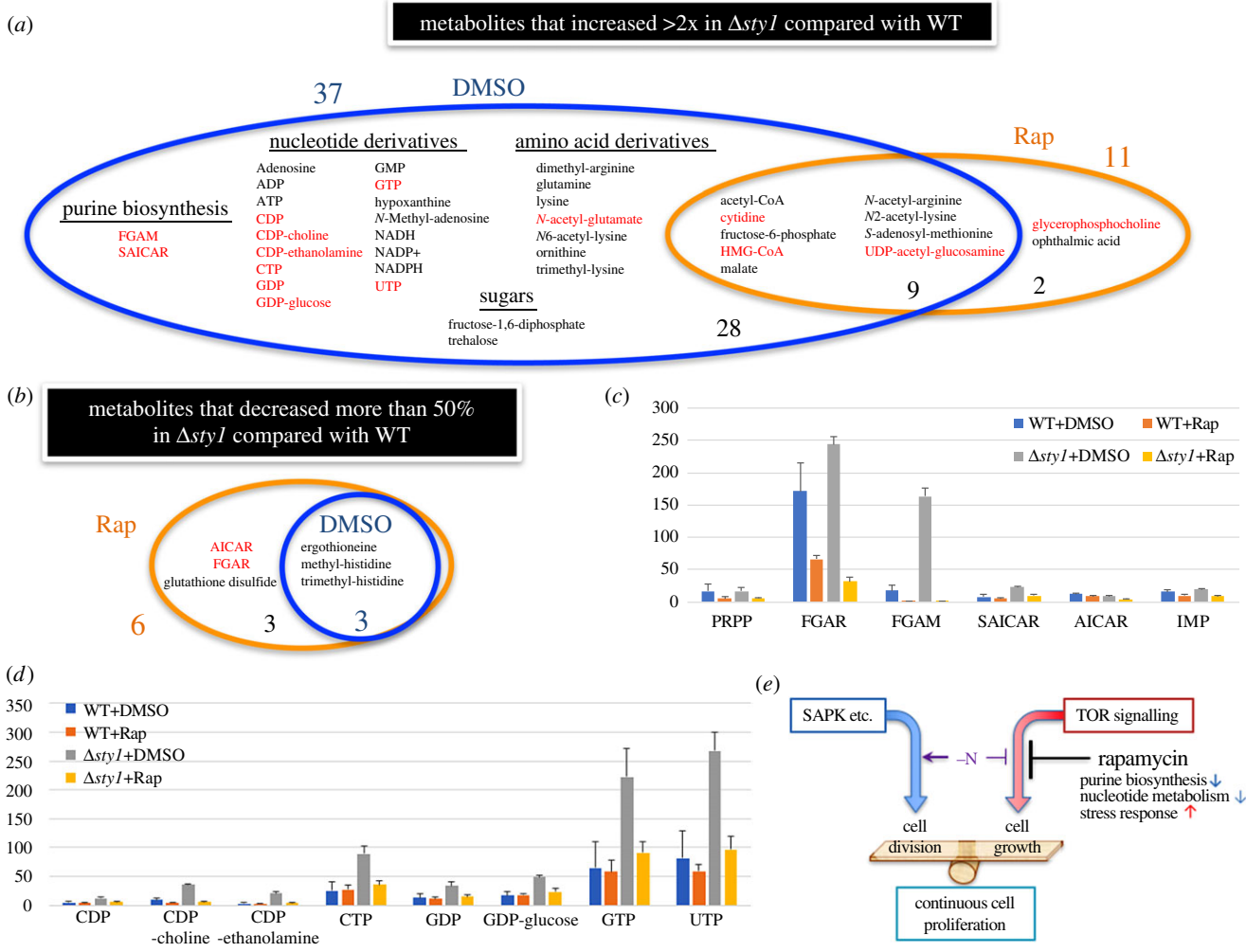
Figure 5. Rapamycin abolished the overproduction of most metabolites in Δ*sty1*. (*a*) Venn diagram of metabolites that increased greater than twofold in Δ*sty1* compared with WT with DMSO or Rap. In the presence of rapamycin, metabolites (in red) decreased to less than 50% of their values when Δ*sty1* was cultured in DMSO. (*b*) Venn diagram of metabolites that decreased more than 50% in Δ*sty1* compared to WT with DMSO or Rap. In the presence of rapamycin, metabolites (in red) decreased to less than 50% of their values when Δ*sty1* was cultured in DMSO. (*c,d*) Normalized mean peak areas with standard deviations of purine bio-synthesis intermediates (*c*) and nucleotide derivatives (*d*) in WT and Δ*sty1* with DMSO or Rap. (*e*) Model of the relationship between identified genes like SAPK and TOR signalling for cell growth and division. If growth and division are well balanced, continuous cell proliferation is maintained. However, if division becomes excessive, as in −N conditions, after several mitotic divisions, continuous proliferation is abandoned. Twelve genes identified in this study may be important for maintaining the appropriate balance.

The most abundant were SAPK mutants, *wis1* and *sty1*, each comprising five ts alleles. Four *wis1* and three *sty1* mutants involved single amino acid substitutions. Further, all but one (*wis1-982*) of these seven missense mutations occurred at conserved amino acids in the catalytic domains of Wis1 and Sty1, strongly suggesting that the loss of function for these protein kinases might be compensated by rapamycin-dependent inactivation of TOR signalling. Thus, the TOR and SAPK signalling pathways seem most likely to have opposing principal cellular functions.

The most striking aspect of suppression of the SAPK Δ*sty1* mutant by rapamycin is that cell viability is restored in both +N and −N media when rapamycin is added (figure 3*d*,*h*), whereas the abnormal rod-like shape of Δ*sty1* cells remains in −N media (figure 3*i*). Furthermore, the DNA content of Δ*sty1* in −N media remains 2C (figure 3*j*), indicating that rapamycin cannot restore G0 phase quiescent cell shape and DNA content. It is thus critically important to determine the rapamycin target for restoring cell viability.

The mechanism of rescue required further investigation. One possibility was suggested by our metabolome analysis,

showing that overproduction of purine biosynthesis inter-mediates and nucleotide derivatives in Δ*sty1* was abolished by rapamycin. In excess, these metabolites in Δ*sty1* cells might cause cell death. Rapamycin especially reduced the level of purine intermediates, like FGAM. In support of such a conclusion, mTORC1 was recently reported to be linked to de novo purine synthesis via the mitochondrial tetrahydrofolate cycle [31]. These are just our initial findings for complex regulation between SAPK and TORC, and we would like to continue more detailed metabolome analyses in future to reveal the mechanisms.

In addition to SAPK, we also identified chromatin regu-lation, vesicle transport and CoA metabolism genes from rapamycin screening. The chromatin regulation group com-prised three genes rescued by rapamycin. Among them, Cut1 and Mis4 are for cohesin release and loading of chromatin, respectively [23,24,32,33], while Htb1 is for nucleosomal his-tone H2B function [25]. Previously, a possible explanation for the rescue of *cut1* mutants by rapamycin was thought to be that the crucial balance between TORC1 and Cut1/separase might prevent premature sister chromatid separation, in

which low TORC1 activity alleviates the Cut1 requirement [19]. However, it may be that in these mutants, the delicate balance between cell elongation and cell division is modulated by rapamycin through its influence over TORC signalling responding to nutritional cues.

The vesicle transport group comprised four genes. Regulation of endosome maturation and endocytosis/exocytosis by TOR signalling and/or rapamycin has been reported [34–38], so some strains rescued by inhibiting the TOR pathway may involve this mechanism.

The metabolism group was related to lipid metabolism and CoA regulation, comprising three genes, Erg10, Fps1 and Cem1. Erg10 catalyses reactions between acetyl-CoA and acetoacetyl-CoA [39]. Both are substrates for the mevalonate pathway to produce geranyl diphosphates for prenylation of Rheb and Rab GTPases [40–42] (figure 2c). Lipids are required for homeostatic synthesis of new membranes during G0 quiescence. TOR signalling is reported to activate the mevalonate pathway via the sterol-responsive element-binding protein (SREBP) [43,44]. Notably, because mrs6 (Rab geranylgeranyl transferase) was also identified in addition to fps1, these metabolism genes could contribute to prenylation of vesicle transport proteins. Cem1 is a beta-keto-acyl synthase that directs the use of acetyl-CoA in fatty acid biosynthesis [45]. These metabolism genes may also work to balance synthesis and degradation of lipids.

Previously, large-scale screening of yeast deletion libraries has been conducted to test rapamycin sensitivity [46,47]. Genes affecting rapamycin sensitivity are mainly involved in upregulation of TOR signalling, as gene deletions cause hypersensitivity to rapamycin. By contrast, our screening employed a ts mutant library in which cell proliferation is disrupted at the restrictive temperature, but is rescued by rapamycin. Rapamycin actions apparently compensate for these deletions and ts mutants. Genes identified in the present study seem to be required to balance TOR signalling for continuous cell proliferation (figure 5e) and raise the possibility of therapeutic applications for rapamycin. Notably, human orthologues of Erg10, Mis4 and Mrs6 are reportedly associated with beta-ketothiolase deficiency, Cornelia de Lange syndrome and intellectual disability, respectively [48–50]. In addition, Cut2/PTTG, a regulator of Cut1/ESPL1, is reportedly associated with cancer [51], while the SAPK cascade is a key therapeutic target of inflammatory disease [52,53]. Our results suggest the potential use of rapamycin to cure or ameliorate these diseases resulting from these genes.

4. Material and methods

4.1. Strains

A collection of 1014 ts mutant strains made by random mutagenesis was used [20]. To identify the mutation responsible for the phenotype, first, a plasmid set containing fragments of an S. pombe genomic library was introduced to each strain. Plasmids that rescued the ts phenotype were sequenced to identify suppressor genes. Second, if suppressor genes were definitive, tetrad analysis was conducted to identify the responsible gene. Or if several suppressor genes were identified, whole-genome sequencing was employed as follows. Mutant strains were backcrossed with WT to collect segregants showing the ts phenotype (ts⁻). DNA samples from several ts⁻ segregants were extracted, mixed equally and sequenced using a Genome Analyzer IIx sequencer (Illumina). Background mutations were eliminated and mutations common to all ts⁻ segregants, which were also identified previously among suppressor plasmids, were confirmed as the responsible genes. The other strain used in this study was h⁻ $\Delta sty1::ura4^+$ ura4-D18 (KS1366) [21] for the $\Delta sty1$ study.

4.2. Screening method and spot test assays

Rough screening of all 1014 strains was conducted using an automated robot system (Biomek FX, Beckman Coulter). Cells were cultivated in YPD liquid media and adjusted to a concentration of 1×10^6 cells ml^{-1}, after which 3 μl were spotted on YPD agar plates with or without 0.1 μg ml^{-1} rapamycin (figure 1a). Plates were incubated at 36°C for 3 days, and colony formation was compared. Subsequent manual spot tests were conducted by cultivating cells to 1×10^7 cells ml^{-1} and serially diluting them in five steps (10-fold dilution in each step). Then 5 μl of each dilution were spotted on new plates. Spotted plates were incubated at 36°C.

4.3. Nitrogen deprivation, cell number, viability assays and flow cytometry

Nitrogen deprivation was accomplished by switching the culture media of exponentially growing cells from EMM2 to EMM2-N (EMM2-N lacks NH$_4$Cl) by vacuum filtration, as described previously [54]. Cell number was measured using a Multisizer3 coulter counter (Beckman Coulter), and cell viability was measured by plating 300 cells on YPD plates and determining the percentage of the number of colonies formed per plated cell. To measure the DNA content, FACS analysis was conducted using a FACSCalibur (Becton Dickinson).

4.4. Microscopy

For DAPI staining, cells were fixed with 2% glutaraldehyde for 10 min on ice, washed 3× with phosphate-buffered saline (PBS), and observed under a fluorescence microscope (Axioplan2, ZEISS) after mixing with DAPI (25 μg ml^{-1}).

4.5. Metabolome analysis

WT and $\Delta sty1$ samples in liquid EMM2 with DMSO or 200 nM rapamycin were incubated for 6 h at 36°C and 40 ml of 5×10^6 cells ml^{-1} were harvested. Metabolome samples were prepared as described previously [55,56] and protein amount for each sample was measured using Direct Detect (Merck). Samples were spiked with two internal standards, PIPES and HEPES, corrected for protein quantity, extracted and separated by liquid chromatography on a ZIC-pHILIC column (Merck), and then measured using an LTQ Orbitrap mass spectrometer (Thermo Fisher Scientific). MZMINE2 software was used for raw mass spectrum analysis [57]. From areas of detected peaks, principal components analyses were calculated and the two principal components were plotted using SIMCA P+ software (Sartorius Stedim) to show clear differentiation of the triplicates under each condition (figure 4b).

Among detected peaks, 95 metabolites were identified by comparing m/z values and retention times with authentic standards. Additionally, FGAM, FGAR and SAICAR were identified as previously explained [56].

References

1. Martel RR, Klicius J, Galet S. 1977 Inhibition of the immune response by rapamycin, a new antifungal antibiotic. *Can. J. Physiol. Pharmacol.* **55**, 48–51. (doi:10.1139/y77-007)

2. Heitman J, Movva NR, Hall MN. 1991 Targets for cell cycle arrest by the immunosuppressant rapamycin in yeast. *Science* **253**, 905–909. (doi:10.1126/science.1715094)

3. Chung J, Kuo CJ, Crabtree GR, Blenis J. 1992 Rapamycin-FKBP specifically blocks growth-dependent activation of and signaling by the 70 kd S6 protein kinases. *Cell* **69**, 1227–1236. (doi:10.1016/0092-8674(92)90643-Q)

4. Brown EJ, Albers MW, Shin TB, Ichikawa K, Keith CT, Lane WS, Schreiber SL. 1994 A mammalian protein targeted by G1-arresting rapamycin-receptor complex. *Nature* **369**, 756–758. (doi:10.1038/369756a0)

5. Sabatini DM, Erdjument-Bromage H, Lui M, Tempst P, Snyder SH. 1994 RAFT1: a mammalian protein that binds to FKBP12 in a rapamycin-dependent fashion and is homologous to yeast TORs. *Cell* **78**, 35–43. (doi:10.1016/0092-8674(94)90570-3)

6. Saxton RA, Sabatini DM. 2017 mTOR Signaling in growth, metabolism, and disease. *Cell* **168**, 960–976. (doi:10.1016/j.cell.2017.02.004)

7. Inoki K, Ouyang H, Li Y, Guan KL. 2005 Signaling by target of rapamycin proteins in cell growth control. *Microbiol. Mol. Biol. Rev.* **69**, 79–100. (doi:10.1128/MMBR.69.1.79-100.2005)

8. Vivanco I, Sawyers CL. 2002 The phosphatidylinositol 3-Kinase AKT pathway in human cancer. *Nat. Rev. Cancer* **2**, 489–501. (doi:10.1038/nrc839)

9. Zhang Y, Gao X, Saucedo LJ, Ru B, Edgar BA, Pan D. 2003 Rheb is a direct target of the tuberous sclerosis tumour suppressor proteins. *Nat. Cell Biol.* **5**, 578–581. (doi:10.1038/ncb999)

10. Kwiatkowski DJ. 2003 Rhebbing up mTOR: new insights on TSC1 and TSC2, and the pathogenesis of tuberous sclerosis. *Cancer Biol. Ther.* **2**, 471–476. (doi:10.4161/cbt.2.5.446)

11. Douros J, Suffness M. 1981 New antitumor substances of natural origin. *Cancer Treat. Rev.* **8**, 63–87. (doi:10.1016/S0305-7372(81)80006-0)

12. Harrison DE *et al.* 2009 Rapamycin fed late in life extends lifespan in genetically heterogeneous mice. *Nature* **460**, 392–395. (doi:10.1038/nature08221)

13. Powers III RW, Kaeberlein M, Caldwell SD, Kennedy BK, Fields S. 2006 Extension of chronological life span in yeast by decreased TOR pathway signaling.

Genes Dev. **20**, 174–184. (doi:10.1101/gad.1381406)

14. Medvedik O, Lamming DW, Kim KD, Sinclair DA. 2007 MSN2 and MSN4 link calorie restriction and TOR to sirtuin-mediated lifespan extension in *Saccharomyces cerevisiae*. *PLoS Biol.* **5**, e261. (doi:10.1371/journal.pbio.0050261)

15. Bjedov I, Toivonen JM, Kerr F, Slack C, Jacobson J, Foley A, Partridge L. 2010 Mechanisms of life span extension by rapamycin in the fruit fly *Drosophila melanogaster*. *Cell Metab.* **11**, 35–46. (doi:10.1016/j.cmet.2009.11.010)

16. Hino K *et al.* 2017 Activin-A enhances mTOR signaling to promote aberrant chondrogenesis in fibrodysplasia ossificans progressiva. *J. Clin. Invest.* **127**, 3339–3352. (doi:10.1172/JCI93521)

17. Yoshida T, Awaya T, Jonouchi T, Kimura R, Kimura S, Era T, Heike T, Sakurai H. 2017 A Skeletal muscle model of infantile-onset pompe disease with patient-specific iPS Cells. *Sci. Rep.* **7**, 13473. (doi:10.1038/s41598-017-14063-y)

18. Nakashima A, Tamanoi F. 2010 Conservation of the Tsc/Rheb/TORC1/S6 K/S6 signaling in fission yeast. *Enzymes* **28**, 167–187. (doi:10.1016/S1874-6047(10)28008-3)

19. Ikai N, Nakazawa N, Hayashi T, Yanagida M. 2011 The reverse, but coordinated, roles of Tor2 (TORC1) and Tor1 (TORC2) kinases for growth, cell cycle and separase-mediated mitosis in *Schizosaccharomyces pombe*. *Open Biol.* **1**, 110007. (doi:10.1098/rsob.110007)

20. Hayashi T, Fujita Y, Iwasaki O, Adachi Y, Takahashi K, Yanagida M. 2004 Mis16 and Mis18 are required for CENP-A loading and histone deacetylation at centromeres. *Cell* **118**, 715–729. (doi:10.1016/j.cell.2004.09.002)

21. Shiozaki K, Russell P. 1995 Cell-cycle control linked to extracellular environment by MAP kinase pathway in fission yeast. *Nature* **378**, 739–743. (doi:10.1038/378739a0)

22. Degols G, Shiozaki K, Russell P. 1996 Activation and regulation of the Spc1 stress-activated protein kinase in *Schizosaccharomyces pombe*. *Mol. Cell Biol.* **16**, 2870–2877. (doi:10.1128/MCB.16.6.2870)

23. Furuya K, Takahashi K, Yanagida M. 1998 Faithful anaphase is ensured by Mis4, a sister chromatid cohesion molecule required in S phase and not destroyed in G1 phase. *Genes Dev.* **12**, 3408–3418. (doi:10.1101/gad.12.21.3408)

24. Murayama Y, Uhlmann F. 2014 Biochemical reconstitution of topological DNA binding by the

cohesin ring. *Nature* **505**, 367–371. (doi:10.1038/nature12867)

25. Maruyama T, Nakamura T, Hayashi T, Yanagida M. 2006 Histone H2B mutations in inner region affect ubiquitination, centromere function, silencing and chromosome segregation. *EMBO J.* **25**, 2420–2431. (doi:10.1038/sj.emboj.7601110)

26. Ahn SH, Cheung WL, Hsu JY, Diaz RL, Smith MM, Allis CD. 2005 Sterile 20 kinase phosphorylates histone H2B at serine 10 during hydrogen peroxide-induced apoptosis in *S. cerevisiae*. *Cell* **120**, 25–36. (doi:10.1016/j.cell.2004.11.016)

27. Bungard D *et al.* 2010 Signaling kinase AMPK activates stress-promoted transcription via histone H2B phosphorylation. *Science* **329**, 1201–1205. (doi:10.1126/science.1191241)

28. Nakashima A, Sato T, Tamanoi F. 2010 Fission yeast TORC1 regulates phosphorylation of ribosomal S6 proteins in response to nutrients and its activity is inhibited by rapamycin. *J. Cell Sci.* **123**, 777–786. (doi:10.1242/jcs.060319)

29. Sajiki K *et al.* 2009 Genetic control of cellular quiescence in *S. pombe*. *J. Cell Sci.* **122**, 1418–1429. (doi:10.1242/jcs.046466)

30. Furuki T, Oku K, Sakurai M. 2009 Thermodynamic, hydration and structural characteristics of alpha,alpha-trehalose. *Front. Biosci.* **14**, 3523–3535. (doi:10.2741/3468)

31. Ben-Sahra I, Hoxhaj G, Ricoult SJ, Asara JM, Manning BD. 2016 mTORC1 induces purine synthesis through control of the mitochondrial tetrahydrofolate cycle. *Science* **351**, 728–733. (doi:10.1126/science.aad0489)

32. Nagao K, Adachi Y, Yanagida M. 2004 Separase-mediated cleavage of cohesin at interphase is required for DNA repair. *Nature* **430**, 1044–1048. (doi:10.1038/nature02803)

33. Uhlmann F, Lottspeich F, Nasmyth K. 1999 Sister-chromatid separation at anaphase onset is promoted by cleavage of the cohesin subunit Scc1. *Nature* **400**, 37–42. (doi:10.1038/21831)

34. Hackstein H, Taner T, Logar AJ, Thomson AW. 2002 Rapamycin inhibits macropinocytosis and mannose receptor-mediated endocytosis by bone marrow-derived dendritic cells. *Blood* **100**, 1084–1087. (doi:10.1182/blood.V100.3.1084)

35. MacGurn JA, Hsu PC, Smolka MB, Emr SD. 2011 TORC1 regulates endocytosis via Npr1-mediated phosphoinhibition of a ubiquitin ligase adaptor. *Cell* **147**, 1104–1117. (doi:10.1016/j.cell.2011.09.054)

36. Rispal D *et al.* 2015 Target of rapamycin complex2 regulates actin polarization and endocytosis via multiple pathways. *J. Biol. Chem.* **290**, 14 963 – 14 978. (doi:10.1074/jbc.M114.627794)

37. Martins RM, Alves RM, Macedo S, Yoshida N. 2011 Starvation and rapamycin differentially regulate host cell lysosome exocytosis and invasion by *Trypanosoma cruzi* metacyclic forms. *Cell Microbiol.* **13**, 943 – 954. (doi:10.1111/j.1462-5822.2011.01590.x)

38. Kim YM, Jung CH, Seo M, Kim EK, Park JM, Bae SS, Kim DH. 2015 mTORC1 phosphorylates UVRAG to negatively regulate autophagosome and endosome maturation. *Mol. Cell.* **57**, 207 – 218. (doi:10.1016/j.molcel.2014.11.013)

39. Hiser L, Basson ME, Rine J. 1994 ERG10 from *Saccharomyces cerevisiae* encodes acetoacetyl-CoA thiolase. *J. Bio.l Chem.* **269**, 31 383 – 31 389.

40. Goldstein JL, Brown MS. 1990 Regulation of the mevalonate pathway. *Nature* **343**, 425 – 430. (doi:10.1038/343425a0)

41. Newman CM, Giannakouros T, Hancock JF, Fawell EH, Armstrong J, Magee AI. 1992 Post-translational processing of *Schizosaccharomyces pombe* YPT proteins. *J. Biol. Chem.* **267**, 11 329 – 11 336.

42. Yang W, Tabancay Jr AP, Urano J, Tamanoi F. 2001 Failure to farnesylate Rheb protein contributes to the enrichment of G0/G1 phase cells in the *Schizosaccharomyces pombe* farnesyltransferase mutant. *Mol. Microbiol.* **41**, 1339 – 1347. (doi:10.1046/j.1365-2958.2001.02599.x)

43. Duvel K *et al.* 2010 Activation of a metabolic gene regulatory network downstream of mTOR complex 1. *Mol. Cell.* **39**, 171 – 183. (doi:10.1016/j.molcel.2010.06.022)

44. Peterson TR *et al.* 2011 mTOR complex 1 regulates lipin 1 localization to control the SREBP pathway. *Cell* **146**, 408 – 420. (doi:10.1016/j.cell.2011.06.034)

45. Harington A, Herbert CJ, Tung B, Getz GS, Slonimski PP. 1993 Identification of a new nuclear gene (CEM1) encoding a protein homologous to a beta-keto-acyl synthase which is essential for mitochondrial respiration in *Saccharomyces cerevisiae*. *Mol. Microbiol.* **9**, 545 – 555. (doi:10.1111/j.1365-2958.1993.tb01715.x)

46. Doi A *et al.* 2015 Chemical genomics approach to identify genes associated with sensitivity to rapamycin in the fission yeast *Schizosaccharomyces pombe*. *Genes Cells* **20**, 292 – 309. (doi:10.1111/gtc.12223)

47. Xie MW, Jin F, Hwang H, Hwang S, Anand V, Duncan MC, Huang J. 2005 Insights into TOR function and rapamycin response: chemical genomic profiling by using a high-density cell array method. *Proc. Natl Acad. Sci. USA* **102**, 7215 – 7220. (doi:10.1073/pnas.0500297102)

48. Fukao T, Mitchell G, Sass JO, Hori T, Orii K, Aoyama Y. 2014 Ketone body metabolism and its defects. *J. Inherit. Metab. Dis.* **37**, 541 – 551. (doi:10.1007/s10545-014-9704-9)

49. Dorsett D. 2007 Roles of the sister chromatid cohesion apparatus in gene expression, development, and human syndromes. *Chromosoma* **116**, 1 – 13. (doi:10.1007/s00412-006-0072-6)

50. Seabra MC, Mules EH, Hume AN. 2002 Rab GTPases, intracellular traffic and disease. *Trends Mol. Med.* **8**, 23 – 30. (doi:10.1016/S1471-4914(01)02227-4)

51. Wang Z *et al.* 2004 Three classes of genes mutated in colorectal cancers with chromosomal instability. *Cancer Res.* **64**, 2998 – 3001. (doi:10.1158/0008-5472.CAN-04-0587)

52. Herlaar E, Brown Z. 1999 p38 MAPK signalling cascades in inflammatory disease. *Mol. Med. Today.* **5**, 439 – 447. (doi:10.1016/S1357-4310(99)01544-0)

53. Kumar S, Boehm J, Lee JC. 2003 p38 MAP kinases: key signalling molecules as therapeutic targets for inflammatory diseases. *Nat. Rev. Drug Discov.* **2**, 717 – 726. (doi:10.1038/nrd1177)

54. Su SS, Tanaka Y, Samejima I, Tanaka K, Yanagida M. 1996 A nitrogen starvation-induced dormant G0 state in fission yeast: the establishment from uncommitted G1 state and its delay for return to proliferation. *J. Cell Sci.* **109**, 1347 – 1357.

55. Pluskal T, Nakamura T, Villar-Briones A, Yanagida M. 2010 Metabolic profiling of the fission yeast S. pombe: quantification of compounds under different temperatures and genetic perturbation. *Mol. Biosyst.* **6**, 182 – 198. (doi:10.1039/b908784b)

56. Sajiki K, Pluskal T, Shimanuki M, Yanagida M. 2013 Metabolomic analysis of fission yeast at the onset of nitrogen starvation. *Metabolites* **3**, 1118 – 1129. (doi:10.3390/metabo3041118)

57. Pluskal T, Castillo S, Villar-Briones A, Oresic M. 2010 MZmine 2: modular framework for processing, visualizing, and analyzing mass spectrometry-based molecular profile data. *BMC Bioinformatics* **11**, 395. (doi:10.1186/1471-2105-11-395)